

RATE OF GROWTH OF BORIDE LAYERS ON STAINLESS STEELS

I. GUNES^{a*}, I. YILDIZ^b

^a*Department of Metallurgical and Materials Engineering, Faculty of Technology, Afyon Kocatepe University, 03 200 Afyonkarahisar, Turkey*
E-mail: igunes@aku.edu.tr

^b*Department of Machine Education, Iscehisar Vocational Schools, Afyon Kocatepe University, 03 200 Afyonkarahisar, Turkey*

ABSTRACT

In this study, the case properties and diffusion kinetics of AISI 310 and AISI 430 steels borided in Ekabor-II powder were investigated by conducting a series of experiments at temperatures of 1123, 1223 and 1323 K for 2, 4 and 6 h. The boride layer was characterised by optical microscopy, X-ray diffraction technique and micro-Vickers hardness tester. X-ray diffraction analysis of boride layers on the surface of the steels revealed the existence of Fe_xB_y , Cr_xB_y and Ni_xB_y compounds. The thickness of boride layer increases by increasing boriding time and temperature for all steels. Depending on the chemical composition of substrates, the boride layer thickness on the surface of the AISI 310 and AISI 430 steels was found to be 50.48 and 91.62 μm , respectively. The hardness of the boride compounds formed on the surface of the AISI 310 and AISI 430 steels ranged from 1658 to 2284 $\text{HV}_{0.1}$ and 1762 to 2165 $\text{HV}_{0.1}$, respectively, whereas Vickers hardness values of the untreated steels AISI 310 and AISI 430 were 276 $\text{HV}_{0.1}$ and 328 $\text{HV}_{0.1}$, respectively. Depending on temperature and layer thickness, the activation energies of boron in 310 and 430 steel were found to be 165.45 and 134.95 kJ/mol, respectively.

Keywords: stainless steel, boride layer, microhardness, kinetics, activation energy.

AIMS AND BACKGROUND

Boriding is a thermochemical surface treatment, in which boron atoms diffuse into the surface of a workpiece to form borides with the base material. When applied to the adequate materials, boronising provides the surfaces with high hardness, wear and abrasion resistance, heat resistance or corrosion resistance¹⁻⁶. But the main advantage

* For correspondence.

of boronising metals is the possibility to alloy a high surface hardness with a low friction coefficient. This leads to a good wear resistance. Because the relationship between the surface hardness and wear rates of the boronised samples also confirms that the wear resistance is improved with the hardness increasing⁷⁻¹⁰.

Process involves heating well-cleaned materials in the range of 700 to 1000°C, preferably for 1 to 12 h, in contact with a boronaceous solid powder, paste, liquid or gaseous medium. The most frequently used method is pack boriding which is similar to pack carburising. The powder-pack boronising is a cost-effective process and has the advantage of simplicity in comparison to other boronising processes¹¹⁻¹³.

Once boron is deposited on the surface, the diffusion rate of boron through the matrix is controlled by the process temperature and time¹³⁻¹⁵. In general, the diffusion rate of boron is higher at higher temperatures, while time is critical for the thickness and composition of the boride layer. Additionally, the chemical composition of the substrate material is another important parameter and plays a major role in boron diffusion¹⁶⁻¹⁸.

The main objective of this study was to investigate the rate of growth of boride layers on stainless steels and the effect of process parameters, such as temperature, time and chemical composition, on the boride layers formed on the AISI 310 and AISI 430 steel after powder pack boriding at different processing temperatures and times.

EXPERIMENTAL

Boriding and characterisation. Table 1 presents the composition of the untreated AISI 310 and AISI 430 steels. The test specimens were cut into Ø 25×8 mm dimensions, ground up to 1000 G and polished using diamond solution. The boriding heat treatment was carried out in a solid medium containing an Ekabor-II powder mixture placed in an electrical resistance furnace operated at the temperature of 1123, 1223 and 1323 K for 2, 4 and 6 h under atmospheric pressure. The microstructures of polished and etched cross-sections of the specimens were observed under a Nikon MA100 optical microscope. The presence of borides formed in the coating layer was confirmed by means of X-ray diffraction equipment (Shimadzu XRD 6000) using Cu K α radiation. The thickness of borides was measured by means of a digital thickness measuring instrument attached to an optical microscope (Nikon MA100). The hardness measurements of the boride layer on each steel and untreated steel substrate were made on the cross-sections using a Shimadzu HMV-2 Vickers indenter with a 100 g load.

Table 1. Chemical composition of test materials (wt.%)

Steels	C	Si	Mn	Cr	Ni
AISI 310	0.25	1.50	0.85	25.0	19.5
AISI 430	0.12	0.90	0.70	16.5	–

Evaluation of the activation energy of the boron diffusion. In order to study the diffusion mechanism, borided AISI 310 and AISI 430 steels were used for this purpose. It is assumed that the boride layers grow parabolically in the direction of diffusion flux and perpendicular to the substrate surface. So, the time dependence of boride layer thickness can be described by equation (1):

$$x^2 = D t \quad (1)$$

where x is the depth of the boride layer (mm), t – the boriding time (s), D – the boron diffusion coefficient through the boride layer. It is a well-known fact that the main factor limiting the growth of a layer is the diffusion of boron into the substrate. It is possible to argue that the relationship between growth rate constant, D , activation energy, Q , and the temperature in Kelvin, T , can be expressed as an Arrhenius equation (equation (2)):

$$D = D_0 \exp(-Q/RT) \quad (2)$$

where D_0 is a pre-exponential constant, Q – the activation energy (J/mol), T – the absolute temperature (K), and R – the ideal gas constant (J/mol K).

The activation energy for the boron diffusion in the boride layer is determined by the slope obtained in the plot of $\ln D$ versus $1/T$, using equation (3):

$$\ln D = \ln D_0 - Q/RT. \quad (3)$$

RESULTS AND DISCUSSION

Characterisation of boride coatings. The cross-section of the optical micrographs of the borided AISI 310 and AISI 430 steels at the temperature of 1123 and 1323 K for 2 and 6 h are shown in Figs 1 and 2. As can be seen the borides formed on the AISI 310 and AISI 430 steel have a smooth and regular morphology. It was found that the coating/matrix interface and matrix could be significantly distinguished and the boride layer had a not columnar structure. Depending on the chemical composition of substrates, the boride layer thickness on the surface of the AISI 310 and AISI 430 steels was found to be 50.48 and 91.62 μm , respectively in Figs 3a, b.

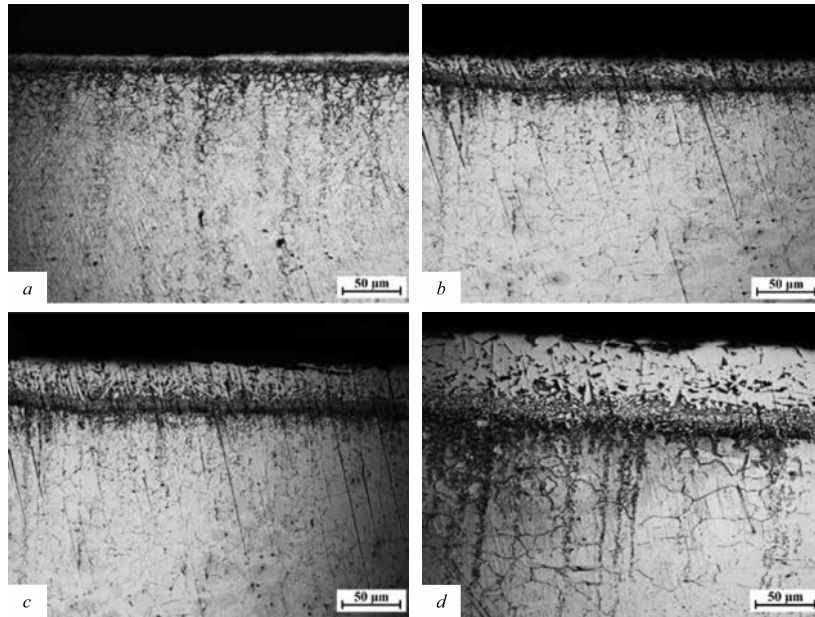


Fig. 1. Cross-section of borided AISI 310 steel: 1123 K – 2 h (a), 1123 K – 6 h (b), 1323 K – 2 h (c), 1323 K – 6 h (d)

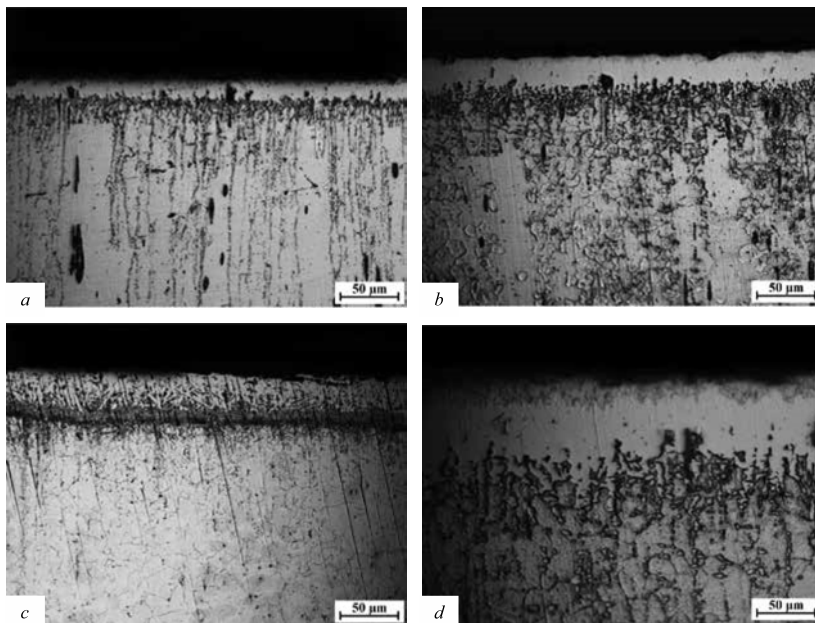


Fig. 2. Cross-section of borided AISI 430 steel: 1123 K – 2 h (a), 1123 K – 6 h (b), 1323 K – 2 h (c), 1323 K – 6 h (d)

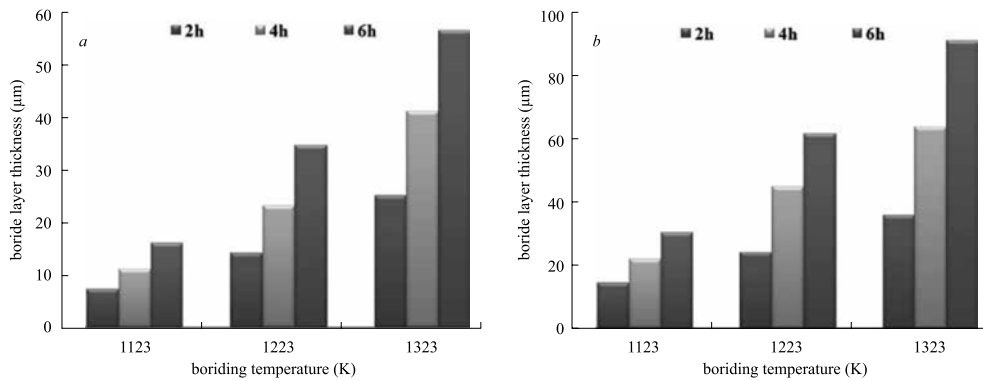


Fig. 3. Thickness values of boride layers with respect to boriding time and temperature: AISI 310 (a), AISI 430 (b)

Figure 4 gives the XRD pattern obtained at the surface of borided AISI 310 and AISI 430 steels at 1123 and 1323 K for treatment time 2 and 6 h. XRD patterns show that the boride layer consists of borides such as MB and M_2B ($M = \text{metal: Fe, Cr, Ni}$). XRD results showed that boride layers formed on the AISI 310 and AISI 430 stainless steels contained FeB, Fe_2B , CrB, Cr_2B , NiB, Ni_2B , Ni_3B and FeB, Fe_2B , CrB, Cr_2B phases, respectively (Figs 4a, b).

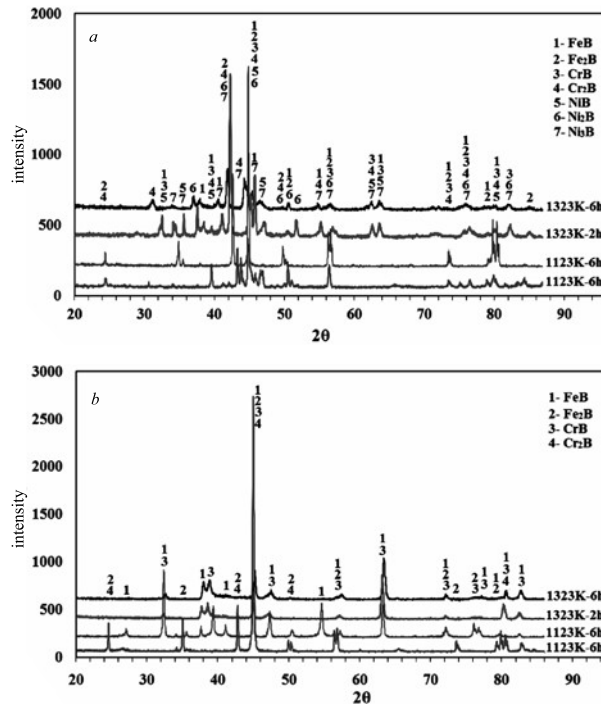


Fig. 4. X-ray diffraction patterns of borided steels: AISI 310 (a), AISI 430 (b)

With increasing time and temperature, Fe_2B phase content decreases and FeB , CrB , NiB phase content increases for AISI 310 steel. The boride layers mainly consist of double intermetallic phase (FeB and Fe_2B) as a result of diffusion of boron atoms from boriding compound to metallic lattice with respect to the holding time.

Microhardness measurements were carried out from the surface to the interior along a line in order to see the variations in the boride layer hardness, transition zone and matrix, respectively. Microhardness of the boride layers was measured at 10 different locations at the same distance from the surface and the average value was taken as the hardness. Microhardness measurements were carried out on the cross-sections from the surface to the interior along a line (Figs 5a, b). The hardness of the boride layer formed on the surface of the AISI 310 and AISI 430 steels ranged from 1658 to 2284 $\text{HV}_{0.1}$ and 1762 to 2165 $\text{HV}_{0.1}$ respectively, whereas Vickers hardness values of the untreated steels AISI 310 and AISI 430 were 276 $\text{HV}_{0.1}$ and 328 $\text{HV}_{0.1}$, respectively. When the hardness of the boride layer is compared with the matrix, boride layer hardness is approximately eight times greater than that of the matrix.

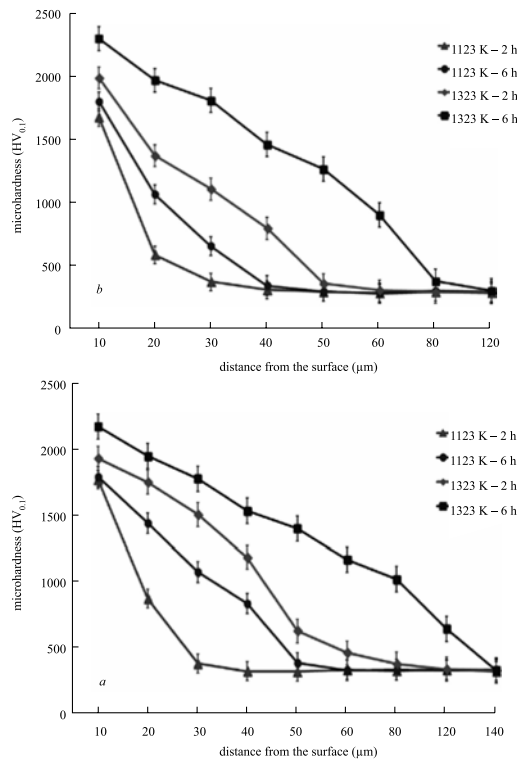


Fig. 5. Variation of hardness depth in the borided steels: AISI 310 (a), AISI 430 (b)

Kinetics. In this study, the effects of the processing temperature and boriding time on the growth kinetics of the boride layer were also investigated. Kinetic parameters

such as processing temperature and time must be known for the control of the boriding treatment. Figure 6 shows the time dependence of the squared value of boride layer thickness at increasing temperatures. This evolution followed a parabolic growth law where the diffusion of boron atoms is a thermally activated phenomenon. The growth rate constant D at each boriding temperature can be easily calculated from equation (1).

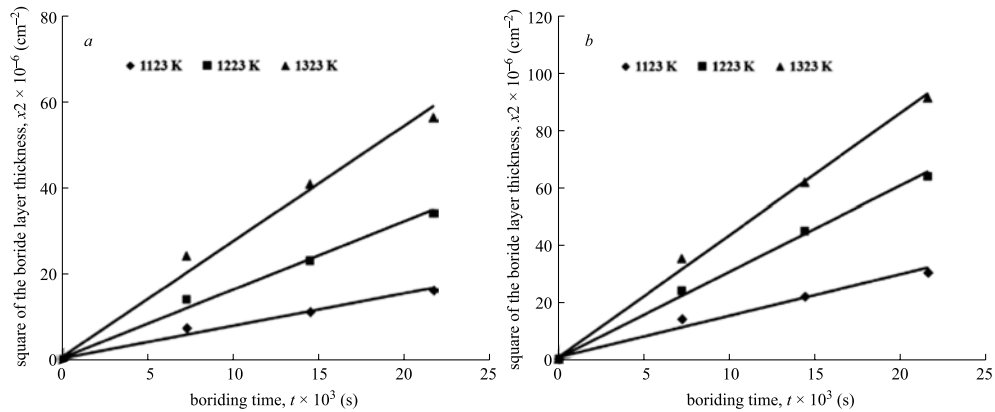


Fig. 6. Time dependence of squared boride layer thickness at increasing temperature: AISI 310 (a), AISI 430 (b)

As a result, the calculated growth rate constants at the three temperatures: 1123, 1223 and 1323 K are the following: 0.42×10^{-10} , 1.80×10^{-10} and $6.16 \times 10^{-10} \text{ cm}^2 \text{ s}^{-1}$ for AISI 310 steel, and 0.12×10^{-9} , 0.40×10^{-9} and $1.89 \times 10^{-9} \text{ cm}^2 \text{ s}^{-1}$ for AISI 430 steel, respectively (Table 2).

Table 2. Growth rate constant (D) as a function of boriding temperature.

Material	Growth rate constant ($\text{cm}^2 \text{ s}^{-1}$)		
	Temperature (K)		
	1123	1223	1323
AISI 310	0.42×10^{-10}	1.80×10^{-10}	6.16×10^{-10}
AISI 430	0.12×10^{-9}	0.40×10^{-9}	1.89×10^{-9}

Figure 7 describes the temperature dependence of the growth rate constant. The plot of $\ln D$ as a function of the reciprocal temperature exhibits a linear relationship according to the Arrhenius equation. The boron activation energy can be easily obtained from the slope of the straight line presented in Figs 7a, b. The value of boron activation energy was then determined as equal to 165.45 kJ/mol for the borided AISI 310 steel and 134.95 kJ/mol for AISI 430 steel.

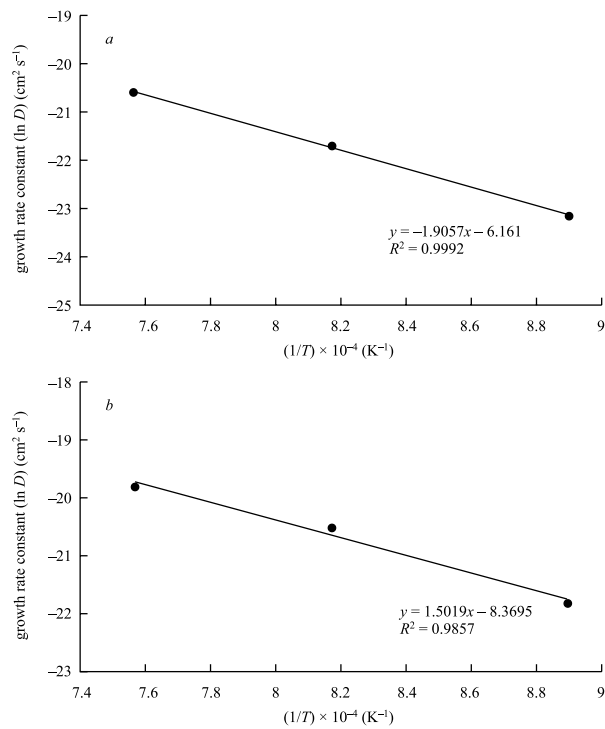


Fig. 7. Temperature dependence of the growth rate constant according to the Arrhenius equation: AISI 310 (a), AISI 430 (b)

The calculated activation energy of AISI 310 is higher than that of AISI 430 due to its high chromium and nickel content. Consequently, diffusion rate of boron atoms perpendicular to surface of AISI 310 is lower than that of AISI 430. The lower activation energy is obtained in the longer layer thickness^{13,18,19}.

Table 3 compares the obtained values of energy with the data found in the literature. It is seen the reported values of boron activation energy depended on the chemical composition of the substrate and on the used boriding method. The calculated value in this study is compatible with the values reported in the literature as seen in Table 3 (Refs 19–21).

Table 3. Comparison of activation energy for diffusion of boron with respect to the different boriding medium and substrates

Steel	Temperature range (K)	Boriding medium	Activation energy (kJ/mol)	References
AISI 304	1073–1223	salt bath	253.35	20
AISI 304	1023–1223	plasma paste	123.00	21
AISI 316	1073–1223	pack	199.00	19
AISI 310	1123–1323	pack	165.45	present study
AISI 430			134.95	

A contour diagram describing the evolution of boride layer thickness as a function of the boriding parameters (time and temperature) is shown in Fig. 8. This contour diagram can be used for two purposes: (1) to predict the coating layer thickness with respect to the process parameters, namely time and temperature; (2) to determine the value of process time and temperature for obtaining a predetermined coating layer thickness^{18,19,22}. The boride layer increased with the increase in boriding time and temperature in the borided both AISI 310 and 430 stainless steel.

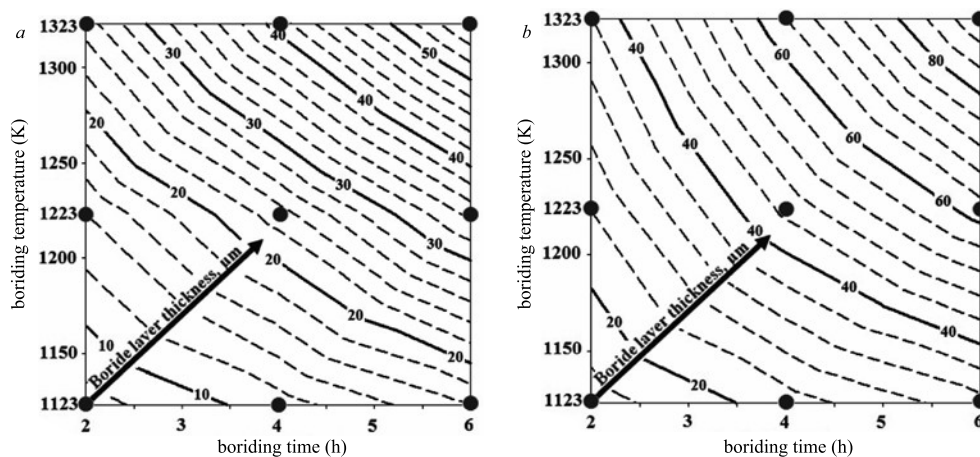


Fig. 8. Contour diagram describing the evolution of boride layer thickness as a function of boriding parameters: AISI 310 (a), AISI 430 (b)

CONCLUSIONS

The following conclusions may be derived from the present study:

- Boride types formed on the surface of the stainless steels have smooth and regular structure.
- The boride layer thickness on the surface of the AISI 310 and AISI 430 steels was obtained, depending on the chemical composition of substrates, 50.48 and 91.62 µm, respectively.
- The multiphase boride coatings that were thermo chemically grown on the AISI 310 and AISI 430 steels were constituted by the FeB, Fe₂B, CrB, Cr₂B, NiB, Ni₂B, Ni₃B and FeB, Fe₂B, CrB, Cr₂B phases, respectively.
- The surface hardness of the borided AISI 310 steel was in the range of 1658–2284 HV_{0.1}, while for the untreated AISI 310 steel substrate it was 276 HV_{0.1}. The surface hardness of the borided AISI 430 steel was in the range of 1762–2165 HV_{0.1}, while for the untreated AISI 430 steel substrate it was 328 HV_{0.1}.
- Activation energy of 134.95 kJ/mol for AISI 430, and 165.45 kJ/mol for AISI 310 steels was determined. It is to claim that diffusivity of B atoms in AISI 310 is lower than that of AISI 430 because of the alloying elements (Cr, Ni) it has.

- A contour diagram relating the boride layer thickness to the boriding parameters (time and temperature) was proposed. It can be used a simple tool to select the optimum boriding layer according to the practical utilisation of this kind of material.

REFERENCES

1. A. K. SINHA: Boriding (Boronising). ASM Handbook, J Heat Treat, (4), 437 (1991).
2. M. KEDDAM: Simulation of the Growth Kinetics of the (FeB/Fe₂B) Bilayer Obtained on a Borided Stainless Steel. Appl Surf Sci, **257**, 2004 (2011).
3. I. GUNES: Tribological Properties and Characterisation of Plasma Paste Borided AISI 5120 Steel. J Balk Tribol Assoc, **20**, 351 (2014).
4. I. CAMPOS-SILVA, M. ORTIZ-DOMINGUEZ, N. LOPEZ-PERRUSQUIA, A. MENESES-AMADOR, R. ESCOBAR-GALINDO, J. MARTINEZ-TRINIDAD: Characterization of AISI 4140 Borided Steels. Appl Surf Sci, **256**, 2372 (2010).
5. I. GUNES: Tribological Behavior and Characterization of Borided Cold-work Tool Steel. Mater Technol, **48**, 765 (2014).
6. S. O. YILMAZ, S. KARATAS: Effect of Mechanical Activation on Jell Boronising Treatment of the AISI 4140. Appl Surf Sci, **275**, 148 (2013).
7. V. SISTA, O. KAHVECIOGLU, G. KARTAL, Q. Z. ZENG, J. H. KIM, O. L. ERYILMAZ, A. ERDEMIR: Evaluation of Electrochemical Boriding of Inconel 600. Surf Coat Tech, **215**, 452 (2013).
8. I. SILVA, M. DOMINGUEZ, O. BARCENAS, M. A. RUIZ, D. BARCENAS, C. QUINTERO, M. Y. REYES: Formation and Kinetics of FeB/Fe₂B Layers and Diffusion Zone at the Surface of AISI 316 Borided Steels. Surf Coat Tech, **205**, 403 (2010).
9. I. GUNES, A. DALAR: Effect of Sliding Speed on Friction and Wear Behaviour of Borided Gear Steels. J Balk Tribol Assoc, **19**, 325 (2013).
10. I. GUNES: Boride Layer Growth Kinetics of the Borided High Alloyed Cold Work Tool Steel. Oxid Commun, **38**, 157 (2014).
11. G. C. EFE, M. IPEK, I. OZBEK, C. BINDAL: Kinetics of Borided 31CrMoV9 and 34CrAlNi7 Steels. Mater Charact, **59**, 23 (2008).
12. G. KARTAL, O. L. ERYILMAZ, G. KRUMDICK, A. ERDEMIR, S. TIMUR: Kinetics of Electrochemical Boriding of Low Carbon Steel. Appl Surf Sci, **257**, 6928 (2011).
13. M. ERDOGAN, I. GUNES: Corrosion Behavior and Microstructure of Borided Tool Steel. Materia-Rio de Janeiro, **20**, 523 (2015).
14. M. KULKA, N. MAKUCH, A. PERTEK, A. PIASECKI: Microstructure and Properties of Borocarburized and Laser-modified 17CrNi6-6 Steel. Optics Laser Tech, **44**, 872 (2012).
15. N. UCAR, O. IYI, A. CALIK, S. KARAKAS: Effect of Ni Content on the Boronising Behaviour of Permalloys. Oxid Commun, **38**, 2 (2015).
16. C. BINDAL, A. H. UCISIK: Characterization of Borides Formed on Impurity-Controlled Chromium-based Low Alloy Steels. Surf Coat Tech, **122**, 208 (1999).
17. B. SARMAN, N. M. TIKEKAR, K. S. RAVI CHANDRAN: Kinetics of Growth of Superhard Boride Layers during Solid State Diffusion of Boron into Titanium. Ceramics Inter, **38**, 6795 (2012).
18. I. GUNES: Kinetics of Borided Gear Steels. Sadhana, **38**, 527 (2013).
19. J. H. YOON, Y. K. JEE, S. Y. LEE: Plasma Paste Boronising Treatment of the Stainless Steel AISI 304. Surf Coat Tech, **112**, 715 (1999).
20. S. TAKTAK: A Study on the Diffusion Kinetics of Borides on Boronized Cr-based Steels. J Mater Sci, **41**, 7590 (2006).
21. O. OZDEMIR, M. A. OMAR, M. USTA, S. ZEYTIN, C. BINDAL, A. H. UCISIK: An Investigation on Boriding Kinetics of AISI 316 Stainless Steel. Vacuum, **83**, 175 (2009).
22. O. KAHVECIOGLU, V. SISTA, O. L. ERYILMAZ, A. ERDEMIR, S. TIMUR: Ultra-fast Boriding of Nickel Aluminide. Thin Solid Films, **520**, 1575 (2011).

Received 22 January 2015

Revised 19 March 2015